2nd International Conference on Autonomous Robots and Agents
December 13-15, 2004 Palmerston North, New Zealand

Safe design and vibration control of a manipulator with passive compliant joints

Munsang Kim*, Seung kook Yun, Sungchul Kang
Intelligent Robotics Research Center, Korea Institute of Science and Technology,
Sungbuk-ku, Seoul 136-791, Korea
{munsang; arumi; kasch}@kist.re.kr

Abstract

: In this paper, design and control of a safe arm with passive compliant joints and visco-elastic covering for a human-friendly service robot are presented. The passive compliant joint (PCJ) is composed of a magneto-rheological (MR) damper and a rotary spring. In an unexpected collision, the joints and covering passively operate and attenuate the applied collision force. Control strategy for this PCJ is also implemented. The rotary spring gives the arm compliant property, and yet it might be a source of vibration. We use the input-preshaping method which is motivated by the input shaping technique(IST) based on impulse response. The result of experiments proves that both of fast motion and force attenuation property of the safe arm can be achieved.

Keywords: Passive Compliant Joint, Magneto-rheological Damper, Visco-elastic Covering, Safety, Input Preshaping, Input shapint Technique

1 Introduction

Robots are recently expected to provide various kinds of services directly to human in human-robot coexisting environment. Considering physical human-robot interaction, safety is one of the most important issues to be accomplished. To make a compliant robot arm can be a good way to greatly enhance the safety performance. Generally there are two strategies to realize the robot compliance: active and passive. Active compliance approach usually makes use of the feedback signals from force/torque sensors equipped either on a robot hand or at joints so that the robot controller may detect the applied external force and generate a proper response. The active compliance approach may have a limit in delayed control and unreliable safety in case of electrical malfunctioning, even though it can offer a high programming ability for compliance control. In this case, a manipulator with active compliance function may cause either damage to human or failure of power transmission due to the shock when unexpected contact occurs. On the other hand, passive compliance can be realized by applying a passive mechanism to produce an appropriate reaction to the applied forces.

There have been several attempts for passive compliance mechanism. Laurin-Kovitz[1] made a programmable passive impedance(PPI) component with an antagonistic nonlinear spring and a binary damper. Morita and Sugano[2] proposed a Mechanical impedance adjuster (MIA) with a variable spring and a pseudo-damper implemented by an electromagnetic brake. Okada[3] used Programmable passive compliance (PPC) shoulder mechanism with a variable-stiffness spring. Yamada[4] made a passive visco-elastic covering. Lim and Tanie[5] proposed a passive joint with a linear spring and a linear damper between a mobile part and an arm .

As shown in the previous work, there are approaches which do not use a covering and cannot attenuate an impact force on unexpected collisions; vibration may occur due to the absence of dampers; implementation is very difficult due to the complexity of the joints. Thus, in this work, a safe arm design overcoming these disadvantages is proposed. Focusing on reliable and safe interaction, this work is a challenge in the passive approach. Especially, the design of the safe arm with a magneto-rheological rotary damper and rotary springs is newly proposed. With this MR damper and rotary springs, a passive compliance joint(PCJ) is developed for the safe arm of a service robot.

The safe arm has advantage in simple compliance control when compared with the arm with active compliance control. When controlling the joint with a PCJ, any additional programming for the control motion program is not needed since the PCJ is inherently passive mechanism. Unless the spring part or the MR damper part is broken mechanically, we can guarantee that compliance control works even if no power is supplied to the electric part of the arm. As well, the compliance control works regardless of the contact point on the arm surface while the arm with active compliance control which uses force/torque sensor at its wrist cannot detect the external force or torque at the contact point of lower links.

In this work impact force in unexpected collisions between a human and a robot is chosen as a safety

condition[6]. From the studies on impact dynamics[7], we can see that factors generating an impulse are the mass, velocity, and joint torque of the arm. Thus to make an arm meet the safety condition, we should basically make a light arm with passive compliant joints and covering, or schedule the velocity according to the inertia value. Developing an arm with passive compliant joints and visco-elastic covering is a main issue.

In human-robot interaction environment, the safe arm has several merits as previously commented. But unwanted vibration may occur because of springs included in each PCJ during the fast motion of each joint. Although the damper of the PCJ may partly suppresses vibration, a fast motion cannot be performed without vibration. This vibration may cause an unstable control or unwanted collision to the environment which degrades safety performance.

The Input Shaping Technique(IST)[8] based on impulse responses has been considered as a good way to solve problem of vibration because of its simple structure and high efficiency. In this paper, we propose an effective method for the vibration control of the safe arm with a properly preshaped trajectory. Although the preshaping method is motivated by the IST based on impulse responses, it has slightly different structure to reduce vibration both at the start and the end position.

With the developed safe arm and the control method of input preshaping, Experiments on the safety and vibration reduction are performed. It is verified that the safe arm meets the safety criteria in the collision test experiment, and vibration reduction can be successfully achieved.

This paper is composed of five sections. In section 2, we introduce how to design the main component of the PCJ and how to integrate components into a PCJ and finally how to design the 6-dof safe arm including three PCJ. And safety evaluation through collision experiment is performed. In section 3, input preshaping method for vibration reduction of the PCJ is proposed as control strategy for the safe arm. And experimental result on the vibration control by proposed input preshaping method is shown. Finally, we conclude this work and some future work are remarked in section 4.

2 Safe arm design

In this section, firstly a passive compliant joint with a magneto-rheological damper and a spring is developed. Second a soft cover is selected. Finally a six-dof arm with the PCJs and cover is designed.

2.1 Passive Compliant Joint Design

The design of the passive compliant joint is depicted in Fig. 1. It consists of a magneto-rheological (MR) rotary damper, a rotary spring for elasticity. The rotary spring has compliant property, but also it might be a source of vibration. Therefore the damper is introduced for damping effect and implemented using the developed MR damper with MR fluid. The PCJ has a resolver sensor with 16-bits high resolution to read the relative position between a reducer and a link due to the spring displacement. The relative position is converted into a relative velocity signal by a numerical differentiation and a filtering and is sent to a damping tuner which converts Coulomb friction property of the MR damper into viscous one. Note that the damper and spring are located in parallel between the reducer and link. The driving unit is composed of a DC motor, an encoder, a timing belt, and a harmonic drive reducer.

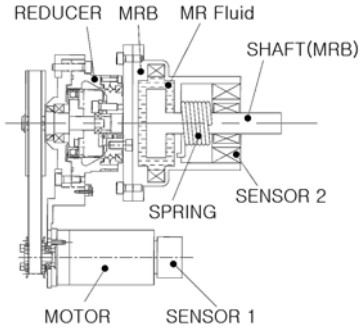

Figure 1: Design of passive compliant joint mechanism.

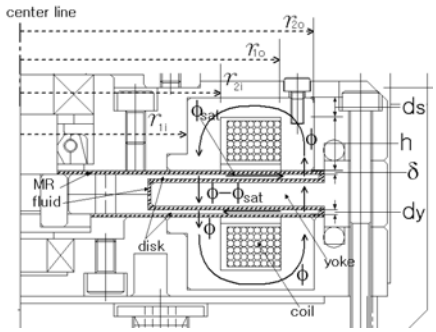

Figure 2: A sectional view of the damper for explaining fluxes in the case that current flows in both coils.

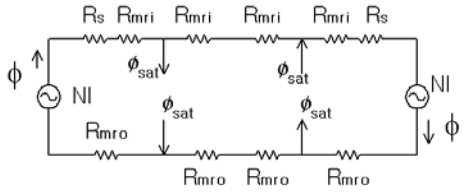

Figure 3: A magnetic circuit considering saturation effects.

Firstly, an MR damper is developed and the experimental tests to the dampers are presented. As shown in Fig. 2, two disks and coils are located in the axial direction because the joints of the arm have margin of length to the direction but a little margin to the radial direction. The hatched area represents MR

fluid (MRF) in the narrow gap. We use the MRF-132LD manufactured by the Lord Corporation [9]. Consider the case that current flows in both coils. Then all magnetic flux through the paths is generated as shown in Fig. 2. And its magnetic circuit considering saturation effects of the disk parts can be obtained as shown in Fig. 3. The reluctance equations for the circuit in Fig. 3 are formulated as follows:

$$R_s = \frac{h + d_s/2}{\mu_0 \mu_{rs}} \left(\frac{1}{A_i} + \frac{1}{A_o} \right) + \frac{(r_{1o} + r_{2o} - r_{1i} - r_{2i})/2}{\mu_0 \mu_{rs} \cdot 2\pi d_s (r_{1o} + r_{2i})/2}, \quad (1)$$

$$R_{mri} = \frac{\delta}{\mu_0 \mu_{rf} A_i}, \; R_{mro} = \frac{\delta}{\mu_0 \mu_{rf} A_o}, \quad (2)$$

$$R_d = \frac{(r_{1o} + r_{2o} - r_{1i} - r_{2i})/2}{\mu_0 \mu_{rs} \cdot 2\pi d_r (r_{1o} + r_{2i})/2}, \quad (3)$$

where R_s, R_{mri}, R_{mro}, R_d are the reluctances of the stator part, left MRF, right MRF, disk part respectively, $\mu_0 (= 4\pi \times 10^{-7})$, $\mu_{rf} (= 6.51)$, $\mu_{rs} (= 1470)$ are the permeability of free space, the relative permeabilities of the MR fluid and steel, and the sectional areas A_i, A_o are calculated as:

$$A_i = \pi (r_{2i}^2 - r_{1i}^2), \; A_o = \pi (r_{2o}^2 - r_{1o}^2). \quad (4)$$

The reluctances of the parts vertical to the disk and yoke are assumed to be zero because they are small. Note that geometrical design parameters for the reluctances are $\delta, h, d_s, d_r, d_y, r_{1i}, r_{2i}, r_{1o}, r_{2o}$. The resultant torque can be calculated from the following equation:

$$Torque = \left[(r_{1i} + r_{2i}) \times (F_{1i} + F_{2i}) + (r_{1o} + r_{2o}) \times (F_{1o} + F_{2o}) \right], \quad (5)$$

where shear forces acting on each sectional areas are as follows:

$$F_{1i} = 80000 B_{1i} A_i - 10000 A_i, \quad (6)$$

$$F_{1o} = 80000 B_{1o} A_o - 10000 A_o, \quad (7)$$

$$F_{2i} = 80000 B_{2i} A_i - 10000 A_i, \quad (8)$$

$$F_{2o} = 80000 B_{2o} A_o - 10000 A_o, \quad (9)$$

and the formula is approximately obtained the data of the Lord Corporation as Fig. 4. The flux density of the disk part is 1.5 (tesla). Thus

$$\phi_{sat} = 1.5 \times 2\pi r_{2i} d_r. \quad (10)$$

By the Kirchoffs's Law for the magnetic circuit,

$$NI = \phi (R_s + R_{mr}) + (\phi - \phi_{sat}) R_{mr}, \quad (11)$$

where

$$R_{mr} = \frac{\delta}{\mu_0 \mu_{rf}} \left(\frac{1}{A_i} + \frac{1}{A_o} \right). \quad (12)$$

Thus

$$\phi = \frac{NI + R_{mr} \phi_{sat}}{R_s + 2R_{mr}}. \quad (13)$$

Finally, the flux densities acting on the each area are calculated as:

$$B_s = \phi / (2\pi r_{2i} d_s), \; B_{1i} = \phi / A_i, \; B_{1o} = \phi / A_o, \quad (14)$$

$$B_{2i} = (\phi - \phi_{sat}) / A_i, \; B_{2o} = (\phi - \phi_{sat}) / A_o. \quad (15)$$

Note that the resultant theoretical torque is calculated from (5).

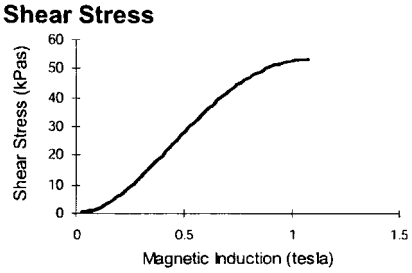

Figure 4: Shear stress versus magnetic flux density of the MRF-132LD [10].

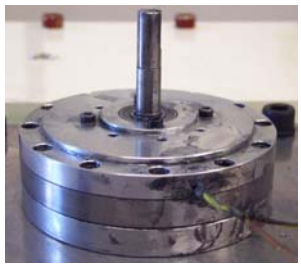

Figure 5: The picture of an implemented damper.

We make three dampers as shown in Fig. 5 for the three joints in the lower part of an arm to be introduced in the section II-C. The numerical parameter values of the dampers can be obtained in [10]. The actual relations between generated torque and applied current using an F/T sensor are experimentally obtained through a setup [11]. The test results are almost linear as shown in Fig. 6.

Resultantly, we can see that the theoretical and experimental torques of the dampers coincides with each other. The detail numerical values of the torques can be obtained in [11].

Now, a technique to tune the damping coefficient is addressed. Originally, the rotary dampers has the Coulomb friction properties, that is, the torque is proportional to the applied current. Thus the relation between the applied current I and torque τ_B of the damper can be approximately represented as follows:

$$\tau_B = slope \times I \times sign(\dot{\theta}_r). \quad (16)$$

Note that a viscous damper should satisfy the following relation:

$$\tau_B = B \dot{\theta}_r, \quad (17)$$

where B is a viscous damping coefficient and θ_r ($\theta_L - \theta_m$) is a relative angle between the link and the output of the reducer. Therefore if we control the current by the following rule

$$I = \frac{B}{slope}\left|\dot{\theta}_r\right|, \qquad (18)$$

the damper can have the viscous damping property. Notice that this property is approximately derived.

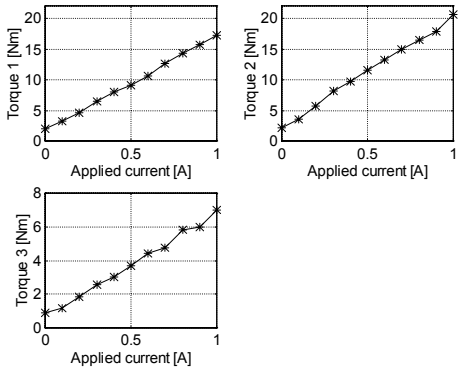

Figure 6: Relations between generated torques and applied currents of the MR dampers.

Secondly, the spring components are explained. Fig. 7 shows a three-dimensional model of the spring component. The upper part and lower part are assembled and rotated relatively. The torsional stiffness of the spring component is calculated as follows:

$$K = n_K k \quad (Nm/rad), \qquad (19)$$

where k is the spring constant of each small spring and n_K is the number of the small springs. Note that the number of the small springs can be tuned. The implemented parameters are given in [11].

(a) (b)

Figure 7: A three-dimensional model of the spring component: (a) lower part, (b) upper part.

Finally, the spring and damper are assembled as Fig. 1 where a cross roller bearing is inserted between the spring and damper. Note that the two components build a parallel structure with a housing. Finally, a passive compliant joint with a housing, a motor, pulleys, a harmonic drive reducer, and a link is obtained. The passive joints are used for the three joints in the lower part of the arm.

Figure 8: The developed safe arm and mobile robot.

2.2 Safe Arm Design

In this subsection, a safe arm with MR-based passive compliant joints and a visco-elastic cover developed in previous subsections is designed for service robot applications. A six-dof safe arm whose payload is 3 (Kg) has been developed as depicted in Fig. 8. This arm is used for the PSR-2 (Public Service Robot) developed at the KIST (Korea Institute of Science and Technology).

2.3 Programmable Damping Effects of the Passive Compliant Joints

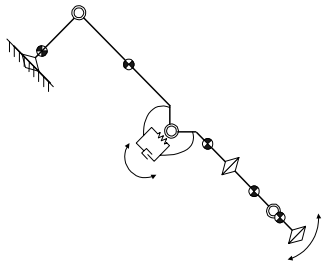

Figure 9: Posture for a test of damping effects.

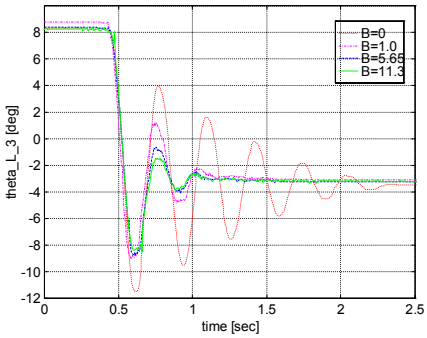

Figure 10: Damped results according to change of B.

The damping effects are evaluated in the posture where the only third joint is set to passive compliant joint as shown in Fig. 9. The first and second axes are fixed and also the input of the harmonic drive of the third axis is fixed. Initially the third joint is set to

about 8.3 (deg) and then released. The resulting responses according to the change of B are obtained as represented in Fig. 10. As the visco-damping coefficient increases, the angle sensed by the 3rd resolver decreases. In steady-state the angle converges to about –3.1 (deg).

2.4 Safety Evaluation through Impact Experiments

A PC-based UMAC motion controller of Delta-Tau ltd. is used for controlling the safe arm, and MR dampers are independently controlled by a separated controller. Each encoder signal is sent to PC via USB and RS-232C port.

Impact experiments are accomplished under the condition where linear velocity is set to 0.2 and 0.5 (m/sec), and $M_H = 9.3$ (Kg) in a posture as shown in Fig. 11. As seen in Fig. 12, impact forces are measured by an F/T sensor, where the solid line indicates impact force in case of 0.5 (m/sec), the dotted line represents one in case of 0.2 (m/sec), and the dash-dotted line indicates the middle limit 100 (N) obtained in [4].

Figure 11: Initial posture for impact experiments.

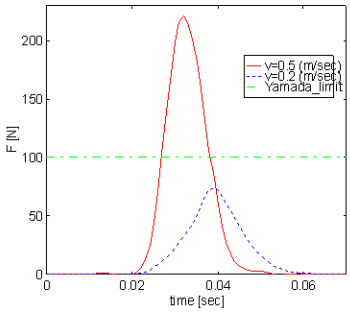

Figure 12: Measured impact forces.

In case of 0.2 (m/sec), the peak force 71 (N) is less than the middle limit. Next, the severity index [11] is calculated to 1.8 by the following equation:

$$SI = \int_0^t a(\tau)^{2.5}\, d\tau \qquad (20)$$

where $a(t) = F(t)/M_H$ and an SI value 400 implies the limit of concussion of the brain [12]. Therefore in view of the two criteria, the arm is safe. Under the condition 0.5 (m/sec), the peak force 212 (N) is greater than the middle limit. Thus the arm is not safe by the Yamada's criterion. But the SI value is calculated to 19 less than 400. Therefore we can see that in view of the severity index the arm is safe in case of 0.5 (m/sec), but in view of the Yamada's criterion the arm is safe only when the impact velocity is less than about 0.25 (m/sec).

3 Input preshaping method for the safe arm

Although the PCJ enables passive compliance for the safe arm, it also can be a source of unwanted vibration. This vibration may cause an unstable control or unwanted collision to the environment. Especially, a lot of residual vibration can occurr during the fast rotation of the PCJ. To cope with this problem, we need a vibration controller for the PCJ. As an effective solution to reduce this vibration, an input preshaping method based on the input shaping technique has been proposed[12].

3.1 With LTI system : 3rd joint control

An experiment of 3rd joint of the safe arm is presented. A desired trajectory is 60 deg/sec during a second. Fig.14 shows the result of the experiment. We can find that there is vibration of 3Hz frequency. The implemented IST reduces vibration of 3rd axis dramatically. The difference between the PCJ displacement of a starting point and steady state is caused by gravity of the link. As shown in Fig.13(c), IST works well even in gravity. A little amount of overshoot shown in Fig.13(c) still remains, but that is due to the inertia of the 3rd link. After the second impulse timing, little vibration is shown.

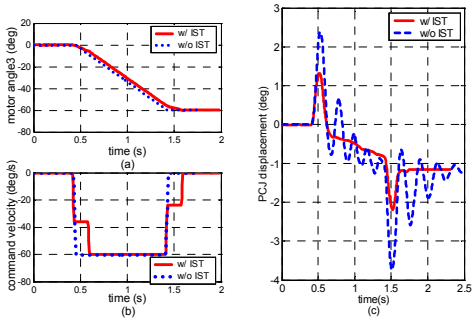

Figure 13: vibration reduction for 3rd axis:

(a) motor angle of the 3rd joint. (b) command velocity of the 3rd motor, (c) PCJ displacement of 3rd PCJ

3.2 With LTV system : 2nd joint control

To prove efficiency of the proposed algorithm, an experiment of 2nd axis with varying inertia is performed. The joint angle of the 2nd joint moves from 30 degree to zero degree, while the joint angle of the 3nd joint rotates from –30 degree to +30 degree as shown in Fig.14. With a given trajectory and the table of period of vibration versus joint configuration, we

can expect that the frequency of vibration varies from 1.85Hz to 1.55Hz. Finally, we can generate the new trajectory by using proposed algorithm. Fig.15 shows the preshaped input and the vibration of the 2nd PCJ. The controller by using the preshaped input clearly suppresses both of vibration including vibration of starting motion and ending motion.

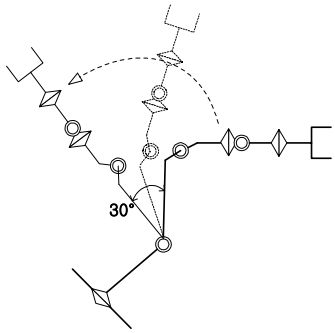

Figure 14: change of joint configuration during the experiment

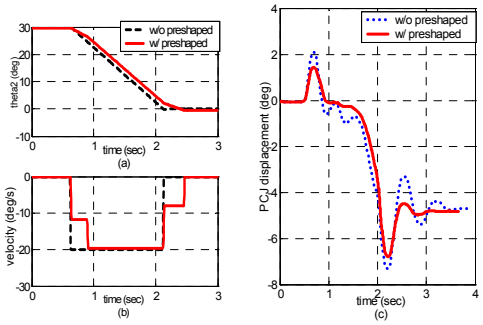

Figure 15: Experiment: vibration reduction for 2nd axis: (a) motor angle of the 2nd joint, (b) command velocity of the 2nd motor, (c) displacement of the 2nd PCJ

4 Conclusion

In this paper, we present a new design of safe arm for service robots with passive compliant joints with springs and dampers and a soft cover. This joint has a feature that a programmable magneto-rheological damper is used. The damper plays a role of suppressing the vibration of the spring. An efficient tuning method to convert the Coulomb friction property of the damper into a viscous damping is proposed. Force attenuation and damping effects of vibration of the arm have been verified through experiments. The joint increases weight by three kilograms per one joint. A proper controller capable of reduction of vibration by input-preshaping method is performed for the safe arm. Experimental results show that proposed method implemented successfully to the safe arm.

5 References

[1] K. F. Laurin-Kovitz, J. E. Colgate, and S. D. R. Carnes, "Design of components for programmable passive impedance," *Proc. of the IEEE International Conference on Robotics and Automation*, pp. 1476-1481, 1991.

[2] T. Morita and S. Sugano, "Development of one-D.O.F. robot arm equipped with mechanical impedance adjuster," *Proc. of the IEEE/RSJ International Conference on Intelligent Robots and Systems*, pp. 407-412, 1995.

[3] M. Okada, Y. Nakamura, and S. Ban, "Design of Programmable Passive Compliance Shoulder Mechanism," *Proc. Of the IEEE International Conference on Robotics and Automation*, pp. 348-353, 2001.

[4] Y. Yamada, K. Suita, K. Imai, H. Ikeda, and N. Sugimoto, "Human-robot contact in the safeguarding space," *IEEE/ASME Transactions on Mechatronics*, vol. 2., no. 4, pp.230-236, 1997.

[5] H.-O. Lim and K. Tanie, "Human safety mechanisms of human-friendly robots: passive viscoelastic trunk and passively movable base," *International Journal of Robotics Research*, vol. 19, no. 4, pp. 307-335, 2000.

[6] Y. Yamada, K. Suita, K. Imai, H. Ikeda, and N. Sugimoto, "Human-robot contact in the safeguarding space," *IEEE/ASME Transactions on Mechatronics*, vol. 2., no. 4, pp.230-236, 1997.

[7] I. D. Walker, "Impact configurations and measures for kinematically redundant and multiple armed robot systems," *IEEE Trans. Robotics and Automation*, vol. 10, no. 5, pp. 670-683, 1994.

[8] N.C. Singer, and W.P. Seering, "Preshaping Command Inputs to Reduce System Vibration," *ASME Journal of Dynamic Systems, Measurement and Control*, Vol.112, pp. 76-82, 1990.

[9] The LORD Corporation, "Magnetorheological fluid MRF-132LD", Product Bulletin, 1999. (http://www.mrfluid.com)

[10] M. Kim, S.-S. Yoon, S. Kang, S.-J. Kim, Y.-H. Kim, H.-S. Yim, C.-D. Lee, I.-T. Yeo, "Safe arm design for service robot," *In Proceedings of The Second IARP -IEEE/RAS Joint Workshop on Technical Challenge for Dependable Robots in Human Environments*, pp. 88-95, 2002.

[11] Society of Automotive Engineers, "Human tolerance to impact conditions as related to motor vehicle design-SAE J885 Jul86," *SAE Handbook (SAE Information Report)*, vol.3, pp. 34.464-34.481, 1999.

[12] S. Yun, S. Kang, M. Kim, S,-S. Yoon, "Input Preshaping Control of the safe arm with MR-based Passive Compliant Joints," *In Proceedings of International Conference on Robotics and Automation*, pp. 2788-2793, 2004.